Article published online: 2024-09-03

Study on the Immunomodulatory effect of Qixian Decoction in an Asthmatic Mice Model Based on Serum Metabolomics

Manman Li[1#] Qingge Chen[2#] Zhenhua Ni[2] Xinyi Le[1] Tong Wu[1*]

[1] National Key Laboratory of Lead Druggability Research, Shanghai Institute of Pharmaceutical Industry Co., Ltd., China State Institute of Pharmaceutical Industry, Shanghai, People's Republic of China
[2] Department of Respiratory Medicine, Putuo Hospital, Shanghai University of Traditional Chinese Medicine, Shanghai, People's Republic of China

Address for correspondence Tong Wu, PhD, National Key Laboratory of Lead Druggability Research, Shanghai Institute of Pharmaceutical Industry Co., Ltd., China State Institute of Pharmaceutical Industry, 285 Copernicus Road, Shanghai 201203, People's Republic of China (e-mail: tongwu88@163.com).

Pharmaceut Fronts 2024;6:e294–e304.

Abstract

The study aimed to investigate the immunomodulatory effect of Qixian Decoction (QXT) in an asthmatic model. In this study, ovalbumin (OVA)-induced asthma in female SPF BALB/c mice was established. Mice were randomly divided into four groups ($n = 8$): a control group, an OVA model group, a low-dose Qixian Granules (KLL) group, and a high-dose Qixian Granules (KLH) group. Mice in the KLL and KLH groups were given the Qixian Granules at a dose of 8 and 16 g/kg, respectively. After the treatment, the lung pathology was evaluated. The expression of inflammatory factors was determined. Serum metabolomics was used to investigate the overall regulation of QXT on the metabolism of asthmatic mice. Our data showed that QXT significantly increased the expression levels of Th1-related interferon-γ, Treg-related interleukin (IL)-10, and transforming growth factor-β1 while decreasing Th1-related tumor necrosis factor α levels in bronchoalveolar lavage fluid, and Th2-related IL-4 and IL-5 levels in serum when compared with the model group (all $p < 0.05$). Serum metabolomics revealed 28 potential biomarkers associated with nine pathways. Compared with the control group, 19 different metabolites in the KLL group and 18 different metabolites in the KLH were reversed. QXT's therapeutic effect against asthma might be related to glycerophospholipid metabolism and arachidonic acid metabolism. In conclusion, QXT could ameliorate inflammation of the OVA-induced asthmatic mice, mainly by regulating the expression of immune-related factors, probably through regulating the Th1/Th2 immune balance and promoting the proliferation of Treg.

Keywords
- asthmatic mice
- serum metabolomics
- Th1/Th2
- Treg
- Qixian Decoction

Introduction

Asthma is a prevalent respiratory disease that is characterized by chronic airway inflammation, airway hyperreactivity, reversible airflow limitation, and airway remodeling. Its occurrence is often associated with genetic and environmental factors. The global prevalence of asthma is on the rise, with an estimated 300 million people worldwide currently suffering from asthma, and these data are expected to rise to 400 million by 2025.[1] In China, the prevalence of asthma

[#] *The authors contributed equally to this work.*

received
March 3, 2024
accepted
August 7, 2024
article published online
September 3, 2024

DOI https://doi.org/10.1055/s-0044-1789576.
ISSN 2628-5088.

Georg Thieme Verlag KG, Rüdigerstraße 14, 70469 Stuttgart, Germany

among people aged 20 and above is 4.2%.[2] The therapies mainly involve the use of glucocorticoids and bronchodilators to reduce inflammation and bronchospasm. However, glucocorticoids have significant side effects and high relapse rates, resulting in poor patient compliance.[3] Recent research has highlighted the involvement of T helper (Th)1, Th2, and regulatory T cell (Treg) cytokines in asthma.[4,5]

Traditional Chinese medicine is safe, reliable, and effective in the treatment of asthma with minimal side effects.[6] The prescription of Qixian Decoction (QXT) is derived from Bufei Decoction and Erxian Decoction[7] and is tailored through the clinical experience of Shanghai Putuo District Central Hospital. The decoction is the traditional dosage form of this prescription, which is not easy to store and carry. However, Qixian Granules can effectively avoid these drawbacks, so the Qixian Granules were used instead of QXT. The composition of Qixian Granules is shown in ►**Table 1**.

Our previous studies have shown that QXT reduced inflammation in airways, and thus exhibited therapeutic effects.[8] However, its roles in regulating Th1/Th2/Treg expression has not been elucidated. From the perspective of modern pharmacology, all the herbs in this formula have anti-inflammatory effects. Astragalus polysaccharide and astragaloside IV are the main ingredients of Huangqi. Astragalus polysaccharide can stimulate and induce the expression of several cytokines and chemokines.[9] Astragaloside IV modulates the differentiation of autoreactive $CD4^+$ T cells and is a potential drug for the treatment of autoimmune diseases.[10] Icariin, the main component of Yinyanghuo, improves lung function and decreases lung inflammation and airway remodeling in mice of ovalbumin (OVA) exposure.[11] Polydatin, the main component of Huzhang, ameliorated interstitial fibrosis and leukocyte infiltration, and decreased alveolar inflammation.[12] The active ingredients of Bajitian,[13] Pipaye,[14] Chuanxiong,[15] Shengdihuang,[16] and Xuanfuhua[17] have anti-inflammatory effects.

The interactions between cell subsets and cytokines have been extensively studied.[18] Researchers have explored the cytokine regulatory function of T cells in encephalitis diseases, and the role of helper T cells in psoriasis.[19] This study aims to assess the effect of QXT on the secretion of inflammatory factors by the cytokines Th1, Th2, and Treg in asthmatic mice. Furthermore, we attempted to determine the anti-inflammatory mechanism of QXT by screening potential endogenous metabolite biomarkers and predicting possible pathways based on serum metabolomics combined with Kyoto Encyclopedia of Genes and Genomes (KEGG) pathway enrichment analysis. We hope to establish the theoretical basis for the treatment of asthma and further research on the pathogenesis of asthma.

Materials and Methods

Experimental Drugs and Reagents

QXT and Qixian Granules were prepared by Shanghai Baolong Pharmaceutical Co., Ltd. (Shanghai, China) in a standardized manner (►**Table 1**). The Chinese medicines were procured in compliance with the Drug Administration Law, the Code of Pharmaceutical Quality Management, and other laws and regulations.

OVA was purchased from Sigma (Sigma, United States). Tumor necrosis factor-α (TNF-α), interleukin (IL)-10, interferon-gamma (IFN-γ), transforming growth factor bata (TGF-β), IL-4, IL-5, and enzyme-linked immunosorbent assay (ELISA) kits were purchased from Multisciences (Hangzhou, China). Potassium aluminum sulfate dodecahydrate was purchased from J&K Scientific.

A sensitizing solution (0.1 g/mL) was prepared by dissolving 0.8 g of potassium aluminum sulfate dodecahydrate in 8 mL of purified water (solution A) followed by 4 mg of OVA in 0.8 mL of physiological saline (solution B). The two solutions were mixed, adjusted pH to 6.5 with sodium hydroxide, allowed to stand for 60 minutes, and then centrifuged for 5 minutes ($750 \times g$). The supernatant was discarded. The residue was re-suspended with physiological saline to the initial volume, which was used immediately. The OVA solution (2 mg/mL) was prepared by dissolving 4 mg of OVA in 2 mL of physiological saline.

Qixian Granules are administered twice daily for adults, with 2 bags per time and 12 g per bag. The clinical dose of medication for mice is calculated based on the equivalent dose of the drug for humans (60 kg). The low dose is the clinical dose. The high dose is twice the clinical dose. In this study, the mice were given Qixian Granules at a low dose of 8 g/kg/d, and a high dose of 16 g/kg/d.

Table 1 The standard formula of Chinese herbal medicine formula entitled Qixian Granules

Chinese name	Pharmaceutical name	Source	Place of production	Weights (%)
Huzhang	*Polygonum cuspidatum* Sieb. et Zucc.	Roots	Jiangxi province	14.71
Huangqi	*Astragalus membranaceus* (Fisch.) Bge.	Roots	Gansu province	14.71
Yinyanghuo/Xianlingpi	*Epimedium brevicornu* Maxim.	Leaves	Gansu province	14.71
Bajitian	*Morinda officinalis* How	Roots	Guangdong province	14.71
Pipaye	*Eriobotrya japonica* (Thunb.) Lindl.	leaves	Jiangxi province	14.71
Shengdihuang	*Rehmannia glutinosa* Libosch.	Roots	Henan province	14.71
Chuanxiong	*Ligusticum chuanxiong* Hort.	Roots	Sichuan province	7.35
Xuanfuhua	*Inula japonica* Thunb.	Flower	Henan province	4.41

Animal Grouping, Modeling, and Intervention

Previous studies have shown that female mice are more prone to developing allergic airway inflammation.[20] Thirty-two healthy female SPF BALB/c mice were purchased from Shanghai SLAC Laboratory Animal Co. (Shanghai, China). The animals were kept in the animal house of the Shanghai Institute of Pharmaceutical Industry (Shanghai, China). Prior to the experiments, the animals were acclimatized for 7 days (humidity $50 \pm 10\%$; temperature $25 \pm 2°C$; 12-hour day/night cycle) with free access to food and drinking water.

As per the previous method,[21] BALB/c mice were randomly divided into four groups ($n = 8$ mice per group): a control group, an OVA model group, a low-dose Qixian Granules (KLL) group, and a high-dose Qixian Granules (KLH) group. The control group was treated with physiological saline, the remaining groups were treated with OVA to establish a mouse model of asthma. The experimental protocol is listed in ►**Fig. 1**. Briefly, mice were sensitized on days 1 and 14 by intraperitoneal injection of sensitizing solution (0.5 mg/mL, 200 µL) and stimulated on days 14, 25, 26, and 27 by nasal drop of OVA solution (2 mg/mL, 50 µL). On days 28 to 41, Qixian Granules (8 g/kg/d) and Qixian Granules (8 g/kg/d) were administered by gavage to the mice in the KLL and KLH groups, respectively. An equal volume of physiological saline was used as a control. On day 42, mice were sacrificed, and the blood, lung tissue, and bronchoalveolar lavage fluid (BALF) were collected. The left bronchi were ligated. The physiological saline (1.5 mL) was instilled into the lungs three times to obtain BALF. The collected BALF was stored at −80°C before the next cytokine analysis. The right lung was fixed in a 4% formaldehyde solution for pathological staining.

Hematoxylin and Eosin Staining and Sirius Red Staining for Pathology

Mice lung tissue was fixed in 4% paraformaldehyde, embedded in paraffin, and sectioned. The nuclei were stained with hematoxylin (Servicebio, Wuhan, China). The cytoplasm and extracellular matrix were stained with eosin (Servicebio, Wuhan, China). Mice's lung tissue was stained with Sirius red (Servicebio, Wuhan, China). The slices were sealed with neutral gum. The pathological condition of mouse lungs was observed and evaluated under a light microscope.

Serum Cytokine Detection

The levels of TNF-α, IFN-γ, IL-10, and TGF-β1 in BALF and IL-4 and IL-5 in serum were determined by ELISA kits according to the manufacturer's instructions.

Serum Metabolomic Analysis

Metabolomics Sample Preparation

Blood was collected and centrifuged for 10 minutes (2,389 × g, 4°C). The serum was collected, 50 µL of which was placed in a 2.0 mL Eppendorf tube, and methanol (150 µL) was added. The mixed solution was shaken for 5 minutes and centrifuged for 10 minutes (18,733 ×g, 4°C). The supernatant was used for mass spectrometry analysis. Quality control (QC) samples are 5 µL aliquots of each sample solution used for method validation.

UPLC-MS/MS Conditions

The chromatographic separation was performed on an ACQUITY UPLC HSS T3 C18 column (100 mm × 2.1 mm, 1.8 µm) using a Waters Acquity ultra-performance liquid chromatography system (Waters, United States). The separations were performed at a steady flow rate of 300 µL/min. Temperature settings of the sample chamber and column oven were 10°C and 35°C, respectively. A full-loop injection mode was used to inject 10 µL of samples. The mobile phases were acetonitrile (B) and water (A) containing formic acid (0.1%, v/v). The mobile phase's gradient was displayed as follows: 0–1.5 minutes, 5–5% B; 1.5–6 minutes, 5–60% B; 6–7 minutes, 60–70% B; 7–18 minutes, 70–95% B; 18–18.1 minutes, 95–5% B; 18.1–20 minutes, 5–5% B.

Mass spectrometry analysis was performed on a Waters XevoG 2 single quadrupole time-of-flight mass spectrometer configured with an electrospray ionization source (Waters, United States) using positive and negative modes. The parameters were described as follows. The mass spectrum scanning ranged from 50 to 1,500 Da. The capillary voltage was set to 3.0 kV/2.5 kV. The ion source temperature was set to 120°C. The nitrogen was used as the desolvation gas at a flow rate of 500 L/h and a temperature of 400°C. Argon was used as the collision gas. Nitrogen was used as the cone gas at a flow rate of 100 L/h and a voltage of 40 V. Low collision energy of 6 eV and high collision energy of 25 to 60 eV are used in MSE mode.

Data Processing Conditions

QC samples were injected six times consecutively to equilibrate the system, then one QC sample was inserted for every five randomly analyzed samples to be tested, followed by one shot of blank methanol to reduce residues.

Data were collected using MassLynx V 4.1 workstation (Waters, Milford, America) and imported into Progenesis QI 2.0 software (Waters, Milford, America) for preprocessing, including mass spectrometry peak extraction, deconvolution, peak alignment, and peak area normalization, to create a data matrix with precise retention time, molecular weight, and peak area. The data matrix was imported into EZinfo 2.0 software (Sartorius, Germany). Multivariate statistical analysis was performed using principal component analysis and orthogonal partial least-squares analysis-discriminant analysis (OPLS-DA) in the pattern recognition method. Endogenous differential metabolite screening was performed by screening variable important in projection ($VIP > 1$), ANOVA (analysis of variance) p-value ($p < 0.05$), and fold change ($FC > 2$ or $FC < 0.5$) and combined with HMDB database search (http://www.hmdb.ca). The identified endogenous differential metabolites were subjected to KEGG-enriched metabolic pathways via the MetaboAnalyst 5.0 database (https://www.metaboanalyst.ca/). The relevant metabolic pathways were analyzed with impact values as the screening condition.

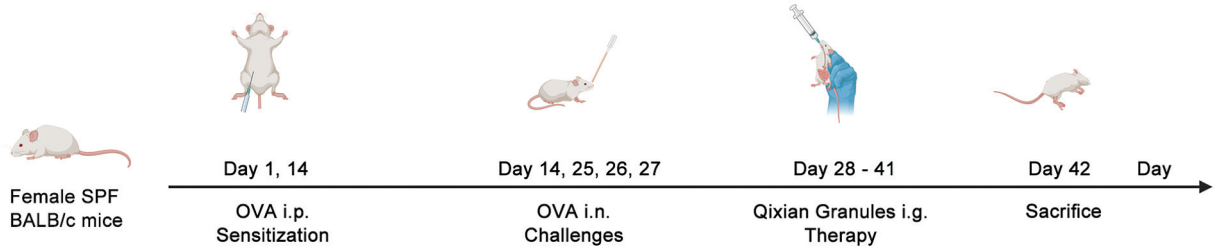

Fig. 1 Schematic diagram of the experimental protocol in mice ($n = 8$).

Statistics of Experimental Results

Statistical analysis was performed using SPSS statistical software (IBM, New York, United States), with all data reported as mean ± standard deviation. One-way ANOVA was used to compare the differences between more than two groups, and a *t*-test was used to compare the differences between two groups. $p < 0.05$ was regarded as statistically significant. Bar graphs were produced and analyzed using GraphPad 8.0 software (GraphPad, California, United States).

Results

Pathological Changes in the Lung Tissue

The HE (hematoxylin and eosin) staining results revealed that the lung tissue of the control group had a normal bronchial structure with no inflammatory cell infiltration, and bronchial and alveolar cavities were clean and free of secretions (►**Fig. 2A**). However, the lung tissue of the model group showed thickening of the smooth muscle layer, edema in the mucosa, high levels of inflammation around the airways and blood vessels, and infiltration of inflammatory cells. With additional KLL and KLH treatment, the pathological changes were alleviated, with the thickening of the bronchial smooth muscle layer, and the secretion and infiltration of inflammatory cells being improved to varying degrees.

Sirius red staining showed that the lung tissue of the control group had a normal bronchial structure, with no abnormal deposition of collagen fibers and thickening of the smooth muscle cell layer in the lung interstitium (►**Fig. 2A**). However, the lung tissue of the model group had significant thickening of the smooth muscle cell layer and deposition of collagen fibers, indicating successful modeling. Compared with the model group, the bronchial fibrosis in the KLL and KLH groups showed different degrees of improvement.

Serum and BALF Inflammatory Factors in Mice

The roles of QXT in regulating asthma-associated inflammatory factors in serum were assessed. Following OVA modeling, serum levels of IL-4 and IL-5 were significantly increased in comparison to the control (►**Fig. 2B**, all $p < 0.05$), indicating successful modeling. After being treated with QXT, serum levels of IL-4 and IL-5 decreased significantly (all $p < 0.01$), suggesting the ability of QXT to improve asthma-related inflammatory factors in serum.

The roles of QXT in regulating asthma-associated inflammatory factors in mouse BALF were further assessed. As shown in ►**Fig. 2B**, after OVA modeling, the levels of TNF-α were significantly increased while the levels of IFN-γ, TGF-β1, and IL-10 were significantly decreased in comparison to the control (all $p < 0.05$). However, the change trends were significantly reversed by additional QXT treatment (all $p < 0.05$).

Metabolomic Analysis

Metabolic Changes between the Groups

The efficacy of QXT in reducing asthma symptoms and possible causes were explored using the OPLS-DA method based on liquid chromatography-mass spectrometry data from serum samples. As shown in ►**Fig. 3**, the groups were well separated, indicating that OVA interference altered serum metabolites and that QXT may have a role in controlling the aberrant metabolic networks.

Identification of Potential Biomarkers in Asthmatic Mice

Distinct clusters of metabolites were observed in control and model mice. Progenesis QI software, and HMDB and KEGG in asthmatic mice were used to screen the potential biomarkers. Significantly different metabolites are identified using FC ratio ≥2 or ratio ≤0.5, VIP ≥1.0, and p <0.05 as screening criteria. As shown in ►**Table 2** and ►**Fig. 4**, there were 28 distinct metabolites in the KLL group compared with the model group, of which 20 metabolites were down-regulated, 6 metabolites were up-regulated, and 19 different metabolites were reversed toward the control group. There were 6 metabolites up-regulated and 19 metabolites down-regulated in the KLH group when compared with the model group, and 18 different metabolites were reversed toward the control group.

Metabolic Pathway Analysis

To explore the metabolic pathway mechanisms associated with asthma, we performed a metabolite enrichment and pathway analysis of 28 differential metabolites using MetaboAnalyst 5.0. The enrichment analysis revealed that these potential biomarkers were associated with nine pathways, including glycerophospholipid metabolism, arachidonic acid metabolism, linoleic acid metabolism, α-linolenic acid metabolism, glycerolipid metabolism, phosphatidylinositol signaling system, biosynthesis of unsaturated fatty acids, primary bile acid biosynthesis, and purine metabolism (►**Table 3** and ►**Fig. 4C**). As shown in ►**Table 3**, QXT

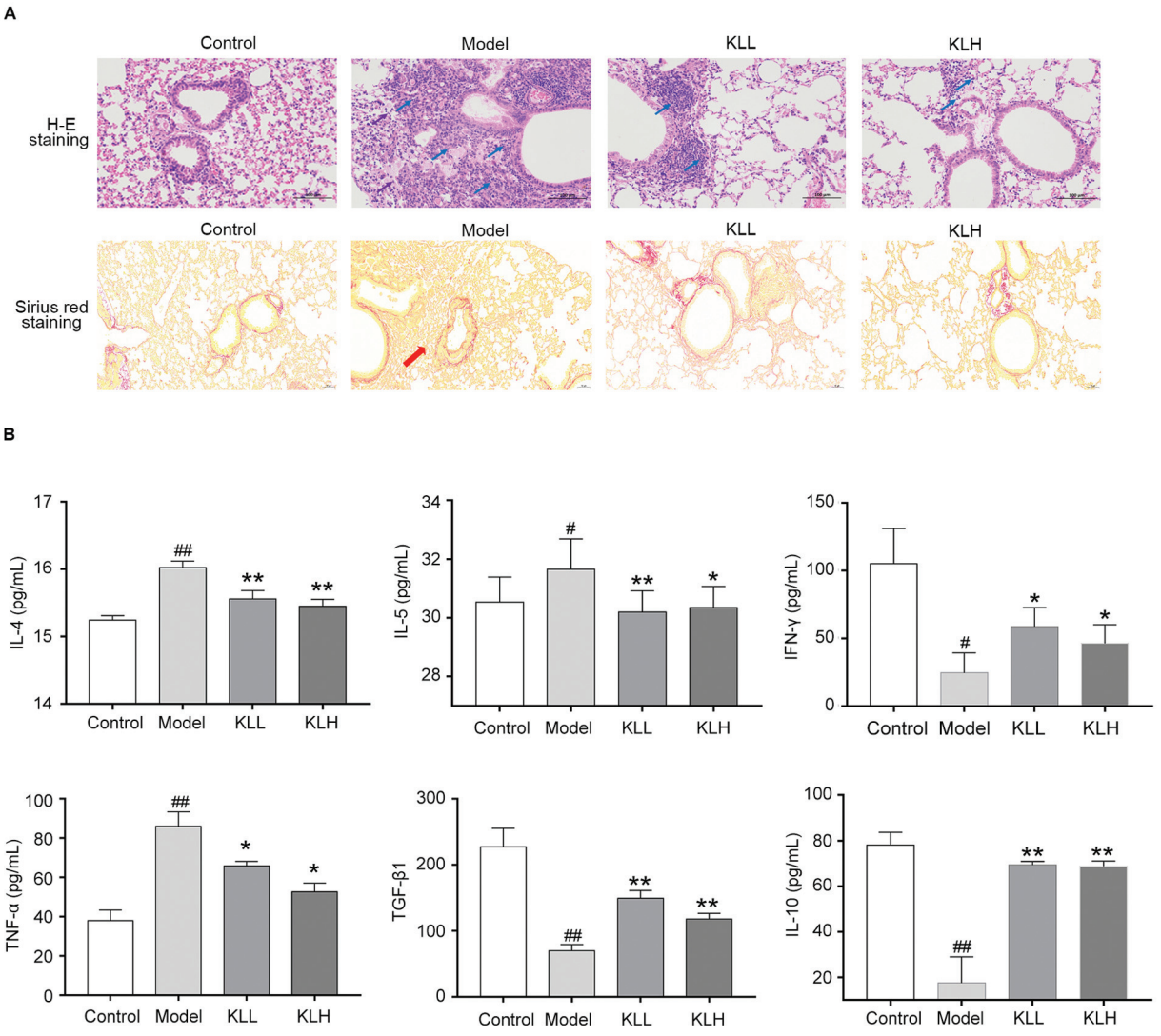

Fig. 2 (**A**) The effect of QXT on lung pathology (magnification, × 200). (**B**) Levels of cytokines IL-4 and IL-5 in serum, as well as the levels of IFN-γ, TNF-α, TGF-β1, and IL-10 in BALF of mice in each group, detected by ELISA kits. Results are represented as mean ± standard deviation ($n = 8$). $^{\#}p < 0.05$, $^{\#\#}p < 0.01$ versus the control group, $^{*}p < 0.05$, $^{**}p < 0.01$ versus the model group. BALF, bronchoalveolar lavage fluid; IFN, interferon; IL, interleukin; TFN, tumor necrosis factor.

significantly altered serum levels of glycerophospholipid metabolism and arachidonic acid metabolism, suggesting that the glycerophospholipid metabolism and arachidonic acid metabolism were key metabolic pathways in asthma. OXT may act through the two pathways.

Discussion

The mechanism of asthma and the targets of QXT are summarized in ►**Fig. 5**. Asthma is an inflammatory disease caused by inhaled allergens (such as pollen, parasites, and cells) that promote type II immune hyperactivation.[22] The pathogenesis is complex and involves a variety of cytokines.[23] Th1 and Th2 cells are subpopulations of $CD4^{+}$ T cells.[24] Th2 cells mediate the humoral immune response, whereas the Th1 cells mediate cellular immunological response. Generally, Th1 and Th2 cells cross-regulate each other through the secretion of cytokines, maintaining a dynamic balance of Th1/Th2 cell function. Evidence suggested that zerumbone regulates the secretion of Th1/Th2 cytokines to reduce allergy responses in a mice model of asthma.[25] Safranal inhibited the degranulation of bone marrow mononuclear cells and suppressed the production of LTC4, TNF-α, and IL-6.[26] Treg cells are essential for controlling Th2 cell activity.[27] Treg is an immunosuppressive T cell that can inhibit the expression of effector T cells, further suppressing inflammation and maintaining the body's immune homeostasis. It is closely associated with asthmatic airway inflammation.[28] IL-10 and TGF-β1 are two hallmark factors secreted by Treg cells,[29] IL-10 inhibits the secretion of various inflammatory factors and the autoimmune response. Serum IL-10 levels are lower in asthma patients than in healthy individuals and are negatively correlated with the severity of the disease.[30]

In asthma, the dendritic cells enter the mediastinal lymph nodes and help to activate helper T cells.[31] The major

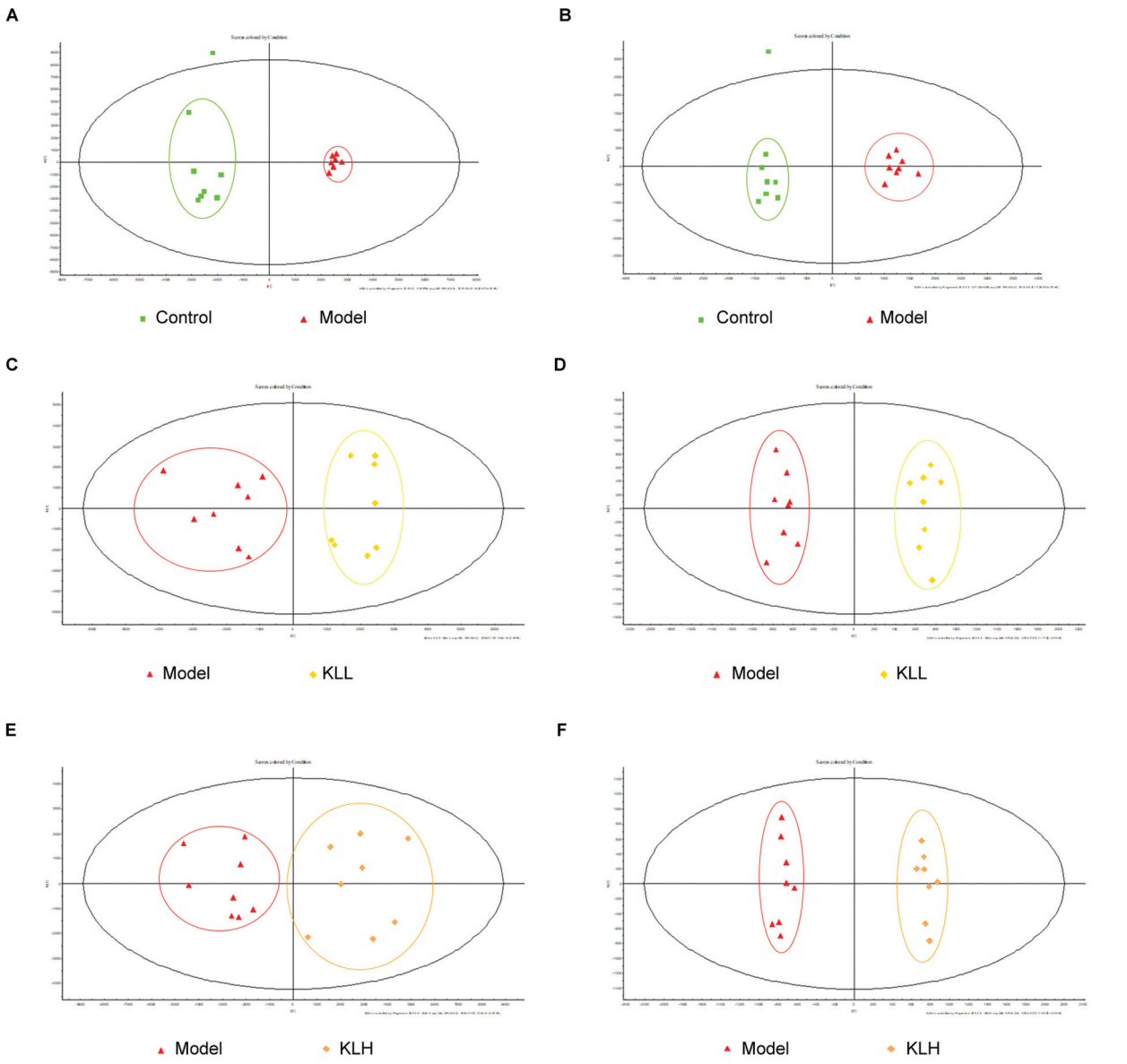

Fig. 3 OPLS-DA score charts between the two groups ($n = 8$ in each group). OPLS-DA score charts in (**A, C, E**) positive mode and (**B, D, F**) negative mode. Colors were used to represent samples from the different groups: control (marked in *green*), model (marked in *red*), KLL (marked in *yellow*), and KLH (marked in *orange*). OPLA-DA, orthogonal partial least squares analysis-discriminant analysis.

histocompatibility complex class II molecule of dendritic cells presents antigenic peptide fragments and co-stimulatory molecules that interact with T cell surface receptors, resulting in a massive production of IL-4 and a Th1/Th2 imbalance.[32] A high level of IL-4 stimulates naive T cell differentiation to Th2, suppressing Th1 cytokine production. Mature Th2 cells secrete various cytokines, including IL-4, IL-5, IL-13, and IL-9. These cytokines play important roles in promoting inflammation and allergic response. IL-4 and IL-13 can induce angiogenesis, which further causes inflammatory cell infiltration. Also, IL-4 and IL-13 can act on B cells, stimulate their differentiation into plasma cells, and increase the secretion of immunoglobulin E (IgE).[33] IL-4, IL-9, and IL-13 enhance the secretion of mucus by cupped cells.[34] IL-5 recruits and enhances the ability of eosinophils to proliferate and differentiate to secrete various cytokines and leukotrienes (LTs). Mast cells, activated by binding IgE and stimulated by IL-9, release histamine, LTs, and prostaglandins.[35] Activation of epithelial cells in asthma also contributes to Th2 cell activation. IL-25 produced by epithelial cells enhances Th2 cell immune memory.[36] IL-33 enhances the ability of Th2 cells to secrete IL-5 and IL-13 and recruit Th2 cells.[37] Thymic stromal lymphopoietin helps Th2 cells to differentiate. In the presence of IFN-γ and IL-12, they boost the differentiation of naive T cells into Th1 cells, which then participate in the cellular immune response by secreting factors such as IFN-γ and TNF-α.[38] IFN-γ, an important inflammatory factor secreted by Th1 cells, counteracts the action of Th2 cells, thereby inhibiting Th2 differentiation and achieving a state of Th1/Th2 homeostasis. TGF-β1 promotes the differentiation of naive T cells toward Treg cells. Treg cells are $CD4^+$ T cells and mainly secrete TGF-β1, IL-10, and other

Table 2 Differential metabolites in the sera of each group

Ion	Metabolite	RT/min	Formula	Model vs. control	KLL vs. model	KLH vs. model
ESI-	Dopamine quinone	5.55	$C_8H_9NO_2$	↑	↓	↓
ESI-	LPC(20:5(5*Z*,8*Z*,11*Z*,14*Z*,17*Z*))	8.02	$C_{28}H_{48}NO_7P$	↑	↑	↑
ESI-	Isofucosterol 3-*O*-[6-*O*-hexadecanoyl-b-*D*-glucopyranoside]	8.15	$C_{51}H_{88}O_7$	↓	↑	↑
ESI-	Tetrahexosylceramide (d18:1/26:0)	9.44	$C_{70}H1_{30}N_2O_{23}$	↓	↑	↑
ESI-	PE(P-16:0e/0:0)	9.82	$C_{21}H_{44}NO_6P$	↑	↓	↓
ESI-	Eicosapentaenoic acid	10.36	$C_{20}H_{30}O_2$	↑	↓	↓
ESI-	Oryzanol C	10.36	$C_{41}H_{60}O_4$	↑	↓	↓
ESI-	PC(15:0/20:3(5Z,8Z,11Z))	10.36	$C_{43}H_{80}NO_8P$	↑	↓	↓
ESI-	LPC (16:0)	10.75	$C_{24}H_{50}NO_7P$	↑	↓	↓
ESI-	Leukotriene A4	10.80	$C_{20}H_{30}O_3$	↑	↓	↓
ESI-	LPA(0:0/18:2(9*Z*,12*Z*))	12.29	$C_{21}H_{39}O_7P$	↑	↓	↓
ESI-	3-Methyl-3-butenyl apiosyl-(1- > 6)-glucoside	15.12	$C_{16}H_{28}O_{10}$	↑	↓	↓
ESI-	Inosine	1.72	$C_{10}H_{12}N_4O_5$	↓	↑	↑
ESI-	Dynorphin B (6–9)	6.97	$C_{26}H_{43}N_{11}O_6$	↑	↓	-
ESI-	LPC(20:4(8*Z*,11*Z*,14*Z*,17*Z*))	8.77	$C_{28}H_{50}NO_7P$	↑	↑	↑
ESI-	17-HDoHE	10.18	$C_{22}H_{32}O_3$	↓	↓	↓
ESI-	Thyrotropin releasing hormone	3.70	$C_{16}H_{22}N_6O_4$	↑	↓	↓
ESI-	PC(15:0/20:4(5Z,8Z,11Z,14Z))	9.34	$C_{43}H_{78}NO_8P$	↑	–	↓
ESI-	9(*S*)-HPODE	9.34	$C_{18}H_{32}O_4$	↑	↓	↓
ESI-	PI(16:0/22:4(10*Z*,13*Z*,16*Z*,19*Z*))	17.67	$C_{47}H_{83}O_{13}P$	↓	↑	↑
ESI-	Cholic acid	6.91	$C_{24}H_{40}O_5$	↑	↓	–
ESI-	Mauritine A	12.04	$C_{32}H_{41}N_5O_5$	↑	↓	–
ESI-	Neuromedin N	12.60	$C_{32}H_{51}N_5O_7$	↑	–	↓
ESI+	PI(22:2(13*Z*,16*Z*)/18:2(9*Z*,12*Z*))	5.63	$C_{49}H_{87}O_{13}P$	↓	↓	↓
ESI+	PE (20:0/24:0)	5.63	$C_{49}H_{98}NO_8P$	↓	↓	↓
ESI+	Ampeloside Bs1	5.63	$C_{45}H_{74}O_{20}$	↓	↓	↓
ESI+	*N*-Undecylbenzenesulfonic acid	14.82	$C_{17}H_{28}O_3S$	↓	↓	↓
ESI+	7-Aminomethyl-7-carbaguanine	14.51	$C_7H_9N_5O$	↓	↓	↓

Note: ↑, up; ↓, down; –, no information available.

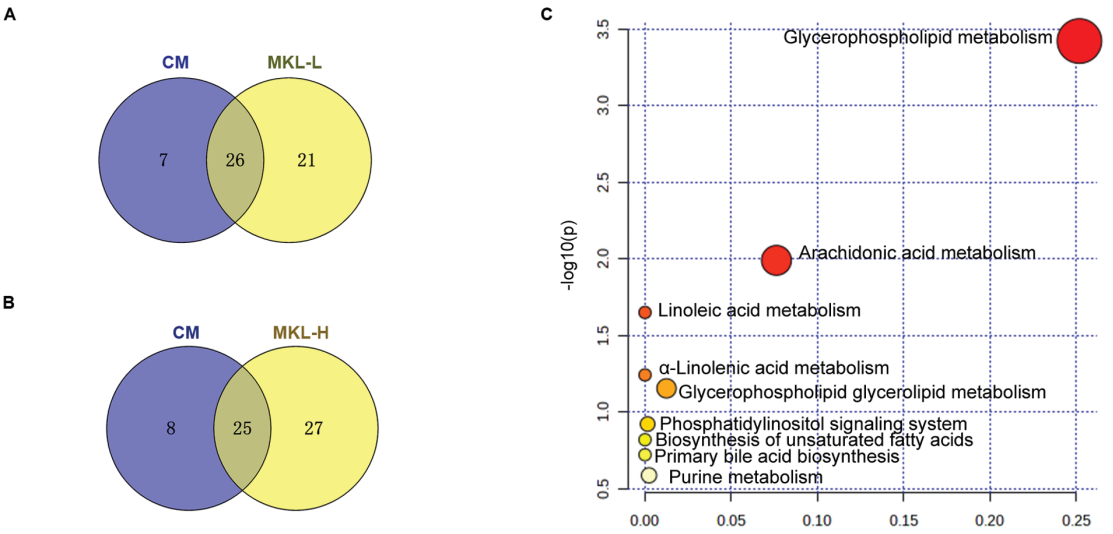

Fig. 4 The Venn diagram of the control, model, and treatment groups. (**A**) Control versus model versus KLL. (**B**) Control versus model versus KLH. (**C**) Summary of the result of MetaboAnalyst pathway analysis.

Table 3 MetaboAnalyst demonstrating the metabolic pathway associated with asthma

Pathway name	Total	Expected	Hits	Raw p	−log(p)	Holm adjust.	FDR	Impact
Glycerophospholipid metabolism	36	0.1626	3	0.0004	3.4222	0.0318	0.0318	0.2517
Arachidonic acid metabolism	36	0.1626	2	0.0102	1.9897	0.8499	0.4301	0.0762
Linoleic acid metabolism	5	0.0226	1	0.0224	1.6496	1	0.6274	0
α-Linolenic acid metabolism	13	0.0587	1	0.0574	1.2414	1	1	0
Glycerolipid metabolism	16	0.0723	1	0.0702	1.1537	1	1	0.0125
Phosphatidylinositol signaling system	28	0.1265	1	0.1200	0.9207	1	1	0.0015
Biosynthesis of unsaturated fatty acids	36	0.1626	1	0.1520	0.8183	1	1	0
Primary bile acid biosynthesis	46	0.2077	1	0.1905	0.7202	1	1	0
Purine metabolism	65	0.2936	1	0.2595	0.5858	1	1	0.0023

anti-inflammatory factors to inhibit effector T cell activation and proliferation.[39] TGF-β1 also inhibits the conversion of T lymphocytes to the Th2 type and reduces eosinophil infiltration by promoting Treg differentiation. It also reduces eosinophil infiltration by promoting Treg differentiation (►**Fig. 5**).[40]

In the present experiment, we found that QXT significantly reduced airway hyperresponsiveness and attenuated the infiltration of inflammatory cells near the small airways in the lungs of asthmatic mice by regulating the secretion of cytokines associated with Th1 and Th2 cells in BALF and serum (►**Fig. 2**). Thus, it was demonstrated that QXT could reduce the inflammation of asthmatic airways by regulating the Th1/Th2 immune balance and promoting the expression of Treg.

Based on impact value ranking, the effect of QXT was mainly related to two metabolic pathways, namely glycerophospholipid metabolism and arachidonic acid metabolism in mouse serum (►**Fig. 6**). Glycerophospholipids are part of the cell membrane. Disturbances in glycerophospholipid metabolism are a key factor in the inflammation that occurs during asthma.[41] Among the metabolites associated with the promotion of asthma, glycerophospholipids account for the

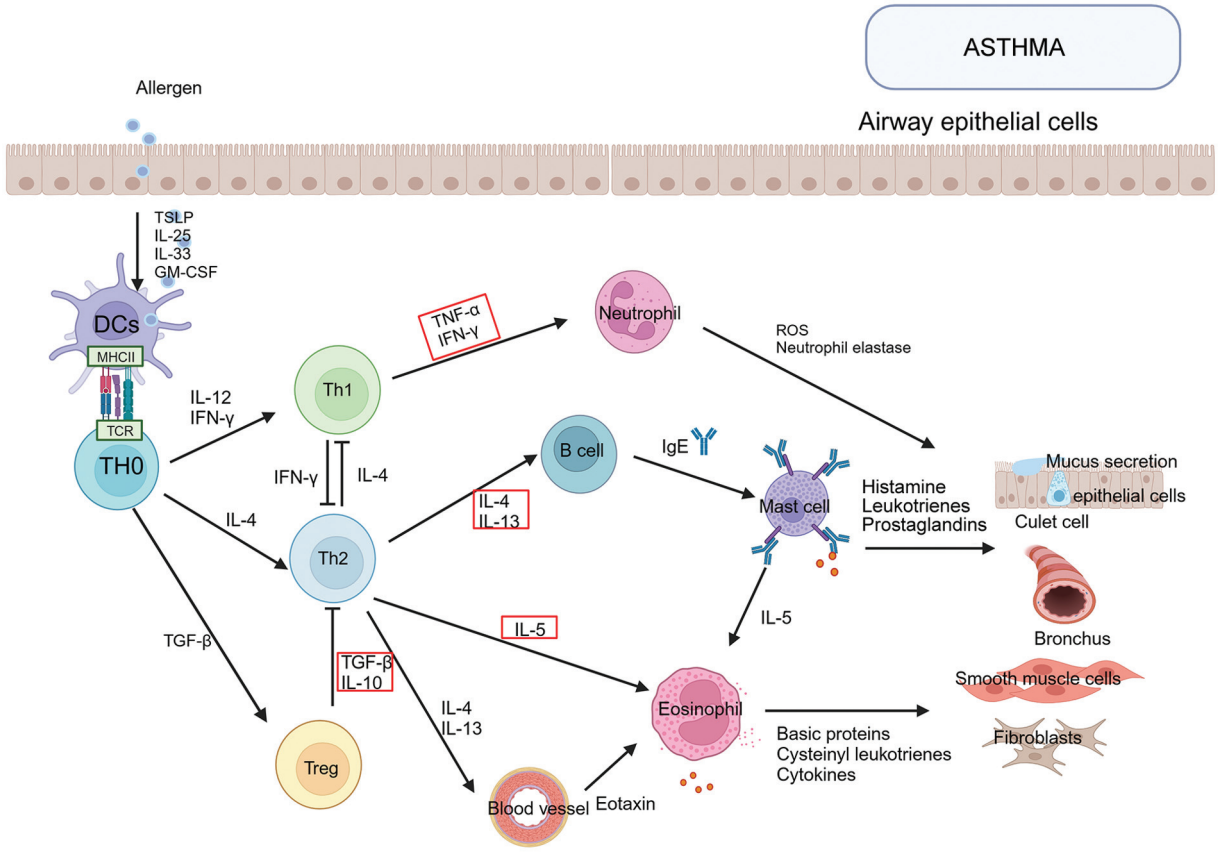

Fig. 5 Diagram of the mechanism of asthma (targets of QXT in *red*). QXT, Qixian decoction. (Created with BioRender.com.)

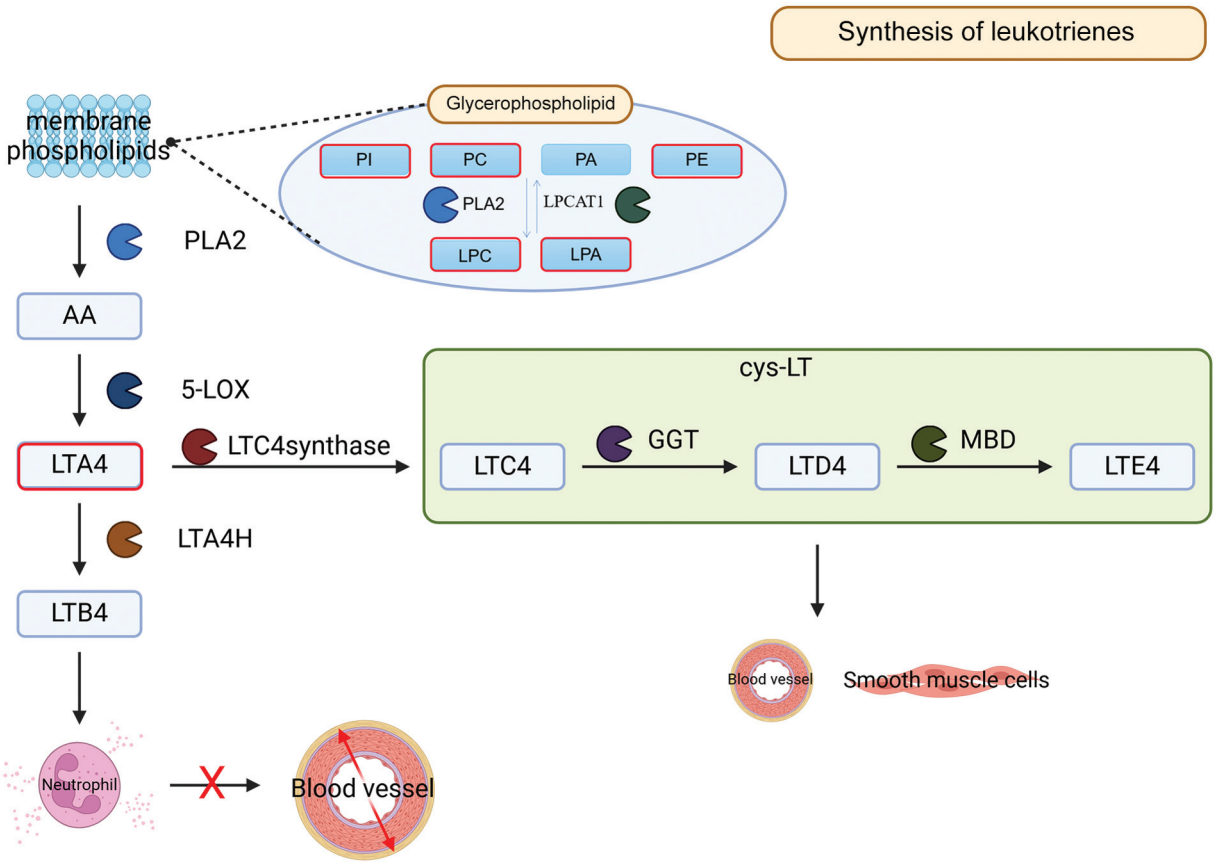

Fig. 6 Network of metabolic pathways significantly altered by QXT treatment. LPA, lysophosphatidic acid; PA, phosphatidic acid; PC, phosphatidylcholine; PE, phosphatidylethanolamine; LPC, lysophosphatidylcholine; PLA2, phospholipase A2.

largest proportion. When glycerophospholipid metabolism is disturbed, lysophosphatidylcholine (LPC) can further induce an inflammatory response in asthma by altering energy metabolism and lipid metabolism. On the one hand, LPC acts as a chemotactic mediator, modifying immune cells by activating specific G protein-coupled receptors. On the other hand, LPC can induce the secretion of the inflammatory factor TNF-α and then participate in the inflammatory process.[42] Lysophosphatidic acid (LPA) is an inflammatory mediator released by the activation of platelets, astrocytes, and other pro-inflammatory cells, and LPA stimulates cytokines such as IL-3 and IL-6 from dendritic glial cells.[43] Phosphatidylcholine (PC) is involved in the development of chronic inflammation in the airways and can cause airway hyperresponsiveness. Phosphatidylethanolamine (PE) and PC can be interconverted.[44] The binding of lipid peroxides to PE can form a novel family of aldehyde-modified PEs as inflammatory mediators, suggesting that the development of inflammation is also associated with elevated PEs.[44] Serum levels of LPC, PE, PC, and LPA were significantly increased in the model group compared with the control group (►**Table 2**), and serum levels of LPC, PE, PC, and LPA in the in the treatment group were significantly regressed, suggesting that QXT can inhibit the inflammatory response by inhibiting the levels of LPC, PC, LPA, and PE. This provides a basis for QXT to treat asthma by regulating the glycerophospholipid metabolic pathway.

During the metabolism of arachidonic acid, particularly the arachidonic acid precursors including prostaglandins, thromboxanes, and LTs. These inflammatory mediators are released via the cytochrome enzyme, cyclooxygenase, and lipoxygenase pathways, respectively. Leukotriene A4 (LTA4) is a transient epoxide intermediate of LTs. LTA4 is synthesized from arachidonic acid by the action of 5-lipoxygenase (5-LOX) and cytosolic phospholipase A 2, which is further metabolized to LTB 4 and LTC 4 by LTA 4 hydrolase (LTA4H) and LTC 4 (►**Fig. 6**).[45] Neutrophils are activated by LTB 4. Neutrophils can rapidly upregulate leukocyte adhesion molecules, promote initial infiltration of neutrophils, induce endothelial cell damage, hinder vascular dilation, exacerbate ischemic tubulointerstitial injury in mice, and ultimately lead to renal tissue damage.[46] Cysteinyl LTs (cys-LT; particularly LTD4) constrict the microcirculation and smooth muscle in the respiratory tract (►**Fig. 6**).[47] The level of LTA4 was increased in the model group compared with the control group and reversed after QXD treatment (►**Table 2**), suggesting that QXT might participate in the arachidonic acid pathway by regulating LTA4 to exert an anti-inflammatory effect.

Serum levels of PC and 9(S)-HPODE were significantly increased in the model group compared with the control group (►**Table 2**), suggesting that QXT can inhibit the inflammatory response by inhibiting the levels of PC and 9 (S)-HPODE.

Conclusion

The present study showed that QXT effectively alleviates allergic airway inflammation in asthmatic mice by regulating the Th1/Th2 immune balance and promoting Treg expression, thereby modulating immune responses. The mechanism of action of QXT might be involved in glycerophospholipid metabolism and arachidonic acid metabolism, which were conducive to regulating immune function and fostering energy production. More studies were encouraged in the future to find the potential links. One limitation of our study was that the potential biomarkers were presumably identified through various databases, therefore experimental validation is needed. These results might contribute to our knowledge of the precise mechanism of action of QXT in asthma mice and offer a foundation for future experiments supporting QXT's clinical use.

Ethical Approval

This research was approved by the Institutional Animal Care and Use Committee of the Pharmacological Evaluation Research Center of the Shanghai Institute of Pharmaceutical Industry (Approval No. SYXK 2019–0027).

Funding

This research was supported by a grant from the Special Project of the Shanghai 2020 "Science and Technology Innovation Action Plan" Biomedical Science and Technology by the Science and Technology Commission of Shanghai Municipality (Grant No. 20S21900700).

Conflict of Interest

None declared.

References

1 Masoli M, Fabian D, Holt S, Beasley RGlobal Initiative for Asthma (GINA) Program. The global burden of asthma: executive summary of the GINA Dissemination Committee report. Allergy 2004;59 (05):469–478
2 Huang K, Yang T, Xu J, et al; China Pulmonary Health (CPH) Study Group. Prevalence, risk factors, and management of asthma in China: a national cross-sectional study. Lancet 2019;394(10196):407–418
3 Agache I, Eguiluz-Gracia I, Cojanu C, et al. Advances and highlights in asthma in 2021. Allergy 2021;76(11):3390–3407
4 Yan X, Liu H, Li T. Lncrna NEAT1 regulates Th1/Th2 in pediatric asthma by targeting MicroRNA-217/GATA3. Iran J Public Health 2023;52(01):106–117
5 Chauhan A, Singh M, Agarwal A, Paul N. Correlation of TSLP, IL-33, and $CD4^+$ $CD25^+$ $FOXP3^+$ T regulatory (Treg) in pediatric asthma. J Asthma 2015;52(09):868–872
6 Wang W, Yao Q, Teng F, Cui J, Dong J, Wei Y. Active ingredients from Chinese medicine plants as therapeutic strategies for asthma: overview and challenges. Biomed Pharmacother 2021; 137:111383
7 Zhang B, Li MY, Luo XM, Wang XB, Wu T. Analysis of the chemical components of Qixianqingming granules and their metabolites in rats by UPLC-ESI-Q-TOF-MS. J Mass Spectrom 2020;55(01):e4484
8 Tang L, Zhu L, Zhang W, et al. Qi-xian decoction upregulated e-cadherin expression in human lung epithelial cells and ovalbumin-challenged mice by inhibiting reactive oxygen species-mediated extracellular-Signal-Regulated kinase (ERK) activation. Med Sci Monit 2020;26:e922003–e1
9 Li CX, Liu Y, Zhang YZ, Li JC, Lai J. Astragalus polysaccharide: a review of its immunomodulatory effect. Arch Pharm Res 2022;45 (06):367–389
10 Xu F, Cui WQ, Wei Y, et al. Astragaloside IV inhibits lung cancer progression and metastasis by modulating macrophage polarization through AMPK signaling. J Exp Clin Cancer Res 2018;37; (01):207
11 Hu L, Li L, Zhang H, et al. Inhibition of airway remodeling and inflammatory response by Icariin in asthma. BMC Complement Altern Med 2019;19(01):316
12 Qiu Y, Pan X, Hu Y. Polydatin ameliorates pulmonary fibrosis by suppressing inflammation and the epithelial mesenchymal transition *via* inhibiting the TGF-β/Smad signaling pathway. RSC Adv 2019;9(14):8104–8112
13 Yu HH, Zhao W, Zhang BX, Wang Y, Li J, Fang YF. Morinda officinalis extract exhibits protective effects against atopic dermatitis by regulating the MALAT1/miR-590–5p/CCR7 axis. J Cosmet Dermatol 2023;22(05):1602–1612
14 Kuraoka-Oliveira ÂM, Radai JAS, Leitão MM, Lima Cardoso CA, Silva-Filho SE, Leite Kassuya CA. Anti-inflammatory and anti-arthritic activity in extract from the leaves of Eriobotrya japonica. J Ethnopharmacol 2020;249:112418
15 Shi J, Li R, Yang S, Phang Y, Zheng C, Zhang H. The protective effects and potential mechanisms of ligusticum chuanxiong: focus on anti-inflammatory, antioxidant, and antiapoptotic activities. Evid Based Complement Alternat Med 2020;2020:8205983
16 Zhang H, Yue Y, Zhang Q, et al. Structural characterization and anti-inflammatory effects of an arabinan isolated from Rehmannia glutinosa Libosch. Carbohydr Polym 2023;303:120441
17 Li J, Guo X, Luo Z, et al. Chemical constituents from the flowers of Inula japonica and their anti-inflammatory activity. J Ethnopharmacol 2024;318(Pt B):117052
18 Dong C. Cytokine regulation and function in T cells. Annu Rev Immunol 2021;39:51–76
19 Hu P, Wang M, Gao H, et al. The role of helper T cells in psoriasis. Front Immunol 2021;12:788940
20 Okuyama K, Wada K, Chihara J, Takayanagi M, Ohno I. Sex-related splenocyte function in a murine model of allergic asthma. Clin Exp Allergy 2008;38(07):1212–1219
21 Tang L, Chen Q, Meng Z, et al. Suppression of Sirtuin-1 increases IL-6 expression by activation of the Akt pathway during allergic asthma. Cell Physiol Biochem 2017;43(05):1950–1960
22 Acevedo N, Alashkar Alhamwe B, Caraballo L, et al. Perinatal and early-life nutrition, epigenetics, and allergy. Nutrients 2021;13 (03):724
23 Komlósi ZI, van de Veen W, Kovács N, et al. Cellular and molecular mechanisms of allergic asthma. Mol Aspects Med 2022;85:100995
24 Fahy JV. Type 2 inflammation in asthma–present in most, absent in many. Nat Rev Immunol 2015;15(01):57–65
25 Shieh YH, Huang HM, Wang CC, Lee CC, Fan CK, Lee YL. Zerumbone enhances the Th1 response and ameliorates ovalbumin-induced Th2 responses and airway inflammation in mice. Int Immunopharmacol 2015;24(02):383–391
26 Cerdá-Bernad D, Costa L, Serra AT, et al. Saffron against neurocognitive disorders: an overview of its main bioactive compounds, their metabolic fate and potential mechanisms of neurological protection. Nutrients 2022;14(24):5368
27 Chen X, Li XM, Gu W, Wang D, Chen Y, Guo XJ. LAT alleviates Th2/Treg imbalance in an OVA-induced allergic asthma mouse model through LAT-PLC-γ1 interaction. Int Immunopharmacol 2017;44:9–15

28 Lloyd CM, Hawrylowicz CM. Regulatory T cells in asthma. Immunity 2009;31(03):438–449
29 Palomares O, Martín-Fontecha M, Lauener R, et al. Regulatory T cells and immune regulation of allergic diseases: roles of IL-10 and TGF-β. Genes Immun 2014;15(08):511–520
30 Böhm L, Maxeiner J, Meyer-Martin H, et al. IL-10 and regulatory T cells cooperate in allergen-specific immunotherapy to ameliorate allergic asthma. J Immunol 2015;194(03):887–897
31 Boonpiyathad T, Sözener ZC, Satitsuksanoa P, Akdis CA. Immunologic mechanisms in asthma. Semin Immunol 2019;46:101333
32 Jiang DB, Zhou YD, Yang XQ, et al. Role of dendritic cells in the pathogenesis of asthma in children [in Chinese]. Zhonghua Er Ke Za Zhi 2004;42(07):520–523
33 Ryzhov S, Goldstein AE, Matafonov A, Zeng D, Biaggioni I, Feoktistov I. Adenosine-activated mast cells induce IgE synthesis by B lymphocytes: an A2B-mediated process involving Th2 cytokines IL-4 and IL-13 with implications for asthma. J Immunol 2004;172 (12):7726–7733
34 Kuperman DA, Schleimer RP. Interleukin-4, interleukin-13, signal transducer and activator of transcription factor 6, and allergic asthma. Curr Mol Med 2008;8(05):384–392
35 Méndez-Enríquez E, Hallgren J. Mast cells and their progenitors in allergic asthma. Front Immunol 2019;10:821
36 Peng B, Sun L, Zhang M, et al. Role of IL-25 on eosinophils in the initiation of Th2 responses in allergic asthma. Front Immunol 2022;13:842500
37 Peebles RS Jr, Aronica MA. Proinflammatory pathways in the pathogenesis of asthma. Clin Chest Med 2019;40(01):29–50
38 Mazzarella G, Bianco A, Catena E, De Palma R, Abbate GF. Th1/Th2 lymphocyte polarization in asthma. Allergy 2000;55 (suppl 61):6–9
39 Bellinghausen I, Khatri R, Saloga J. Current strategies to modulate regulatory T cell activity in allergic inflammation. Front Immunol 2022;13:912529
40 Braga M, Quecchia C, Cavallucci E, et al. T regulatory cells in allergy. Int J Immunopathol Pharmacol 2011;24(1, suppl):55S–64S
41 Zeng C, Wen B, Hou G, et al. Lipidomics profiling reveals the role of glycerophospholipid metabolism in psoriasis. Gigascience 2017;6 (10):1–11
42 Bansal P, Gaur SN, Arora N. Lysophosphatidylcholine plays critical role in allergic airway disease manifestation. Sci Rep 2016;6(01): 27430
43 Oude Elferink RP, Bolier R, Beuers UH. Lysophosphatidic acid and signaling in sensory neurons. Biochim Biophys Acta 2015;1851 (01):61–65
44 van der Veen JN, Kennelly JP, Wan S, Vance JE, Vance DE, Jacobs RL. The critical role of phosphatidylcholine and phosphatidylethanolamine metabolism in health and disease. Biochim Biophys Acta Biomembr 2017;1859(9, Pt B):1558–1572
45 Murphy RC, Gijón MA. Biosynthesis and metabolism of leukotrienes. Biochem J 2007;405(03):379–395
46 He R, Chen Y, Cai Q. The role of the LTB4–BLT1 axis in health and disease. Pharmacol Res 2020;158:104857
47 Kanaoka Y, Austen KF. Roles of cysteinyl leukotrienes and their receptors in immune cell-related functions. Adv Immunol 2019; 142:65–84